



OPEN ACCESS

EDITED BY

S. Hassan HosseinNia,
Delft University of Technology, Netherlands

REVIEWED BY

Mehmet Akif Koç,
Sakarya University of Applied Sciences, Türkiye
Saleh Mobayen,
University of Zanjan, Iran

*CORRESPONDENCE

Xuefeng Leng,
✉ leng2023126@126.com

RECEIVED 03 July 2024

ACCEPTED 13 November 2024

PUBLISHED 10 December 2024

CITATION

Leng X (2024) Second-order sliding mode optimization control of an inverted pendulum system based on fuzzy adaptive technology. *Front. Mech. Eng.* 10:1458852. doi: 10.3389/fmech.2024.1458852

COPYRIGHT

© 2024 Leng. This is an open-access article distributed under the terms of the [Creative Commons Attribution License \(CC BY\)](https://creativecommons.org/licenses/by/4.0/). The use, distribution or reproduction in other forums is permitted, provided the original author(s) and the copyright owner(s) are credited and that the original publication in this journal is cited, in accordance with accepted academic practice. No use, distribution or reproduction is permitted which does not comply with these terms.

Second-order sliding mode optimization control of an inverted pendulum system based on fuzzy adaptive technology

Xuefeng Leng*

School of Intelligent Control, Changzhou Vocational Institute of Industry Technology, Changzhou, China

Introduction: This paper aims at the control problem of nonlinear systems with uncertainty in general, and avoids the deviation of sliding mode controller from the preset constraint region during the convergence process.

Methods: A sliding mode control method based on fuzzy adaptive technique was proposed by constructing obstacle Lyapunov function (BLF). Design problem of fuzzy adaptive second-order sliding mode controller considering output constraints. The Lyapunov function of the cutting barrier is designed, and the fuzzy adaptive second-order sliding mode controller is constructed by combining the Lyapunov function with the regression method. A second-order finite output sliding mode controller is designed for the inverted pendulum system. In the case of unknown external disturbance, the mathematical modeling and force analysis of the first order inverted pendulum system are carried out, and the design problem of the fuzzy adaptive second-order sliding mode controller with output restriction is studied.

Results and Discussion: The proposed fuzzy adaptive second-order sliding mode controller has a good control effect in the inverted pendulum system. The fuzzy adaptive second-order controller stabilizes the sliding mode at 0.1 in 1.25 s, while the fuzzy adaptive second-order controller makes the system state reach equilibrium in 15 s. The accuracy of fuzzy adaptive second-order sliding mode controller reaches 99.2%, which is superior to other methods in terms of balance accuracy and recall rate. The controller not only has a fast response speed, but also can effectively suppress system flutter and ensure the rapid stability of the system after constraints. This research method lays a foundation for the design of fuzzy adaptive sliding mode control algorithm.

KEYWORDS

fuzzy logic, adaptive, inverted pendulum, sliding mode controller, system

1 Introduction

Non-linear systems are widely used in practical complex engineering, often exhibiting characteristics of multi-variable, high-order, and strong coupling. The internal uncertainty and external interference make the traditional control methods difficult to deal with, resulting in system performance degradation and even instability (John et al., 2023). In practice, the changes in system parameters and external environmental disturbances inevitably affect the control effect, so it is very important to develop a robust control method that can adapt to uncertainty.

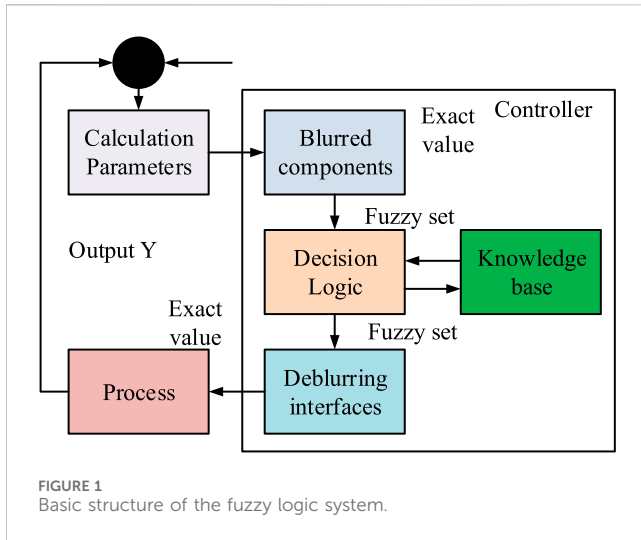


FIGURE 1 Basic structure of the fuzzy logic system.

As a classical control theory verification platform, the inverted pendulum system is often used to test and verify the effectiveness of control algorithms due to its under-actuation, non-linearity, and instability (Kavikumar et al., 2022; Zare et al., 2022). SMC, also known as variable structure control, is a special form of non-linear control characterized by the discontinuity of control. The main difference of the sliding mode controller (SMC) lies in its ability to dynamically adjust the system structure, guiding the system to move along the designed sliding trajectory (Fei et al., 2022). In addition, SMC is widely used in non-linear control fields, such as robot control, path tracking, and motor control, thus becoming an important control method in the field of automatic control (Wu et al., 2022). Qiao and Wang artificially enhanced the speed control effect of the direct drive system of permanent magnet synchronous motors using a gentle conversion function instead of the conventional switching function. An SMC based on fuzzy logic was constructed. Through simulation experiments, the controller was validated in handling sudden loads and simulating actual operating loads. Compared with traditional SMC, its overshoot was smaller and its robustness was better (Qiao and Wang,

2024). Chen et al. put forward an adaptive SMC to address the challenges of conventional SMC in jitter and obtaining sliding surface derivative data. Sliding mode variables were incorporated into the super twisting algorithmic parameters while retaining the discontinuous terms within the integrated function to reduce system vibration. This research method significantly improved the side slip angle compared with traditional SMC (Chen et al., 2024). Sun et al. put forward a hybrid controlling scheme that integrated the torque allocation method and SMC technology to reduce torque fluctuations and improve the dynamic response efficiency. SMC was improved to further reduce torque fluctuations at high speeds and accelerate the response speed. It enhanced the system adaptability and verified the effectiveness of the hybrid control scheme (Sun et al., 2022).

Dong et al. put forward a stepped SMC using Lagrange law to avoid accidents caused by oscillation during container handling. Its steady state was established using Lyapunov's theorem and Babarat's theorem. This research method quickly reduced swing and attitude tilt, which had good fault tolerance for parameter changes (Dong et al., 2023). Zhao et al. proposed a non-singular fast SMC strategy that combined adaptive algorithms and super distortion technology to reduce the impact of disturbances on the permanent magnet linear synchronous motor servo system. A control rule for stable convergence of position signals was constructed. The control method effectively improved control accuracy and system anti-interference performance (Zhao et al., 2023). Mendoza et al. proposed a small UAV trajectory tracking control method based on the FANPID controller. The method used the adaptive characteristics of the FANPID-Lyapunov controller to estimate the rotation angle. The UAV parameters were identified by the fuzzy adaptive neuron method. The simulation results showed that the control system had advantages in self-tuning and optimization, and the error was significantly reduced compared with other PID controllers (Mendoza and Yu, 2023). Chen et al. put forward a novel tracking means for autonomous vehicles. An adaptive system adjusted the SMC gain to ensure accurate and stable tracking of vehicle speed under various conditions. After simulation verification, the proposed scheme had significant advantages compared with other existing control strategies (Chen et al., 2022). Moudoud et al. put forward a fuzzy adaptive SMC for tracking to address the uncertainty and disturbance issues faced by electric wheeled robots. This controller

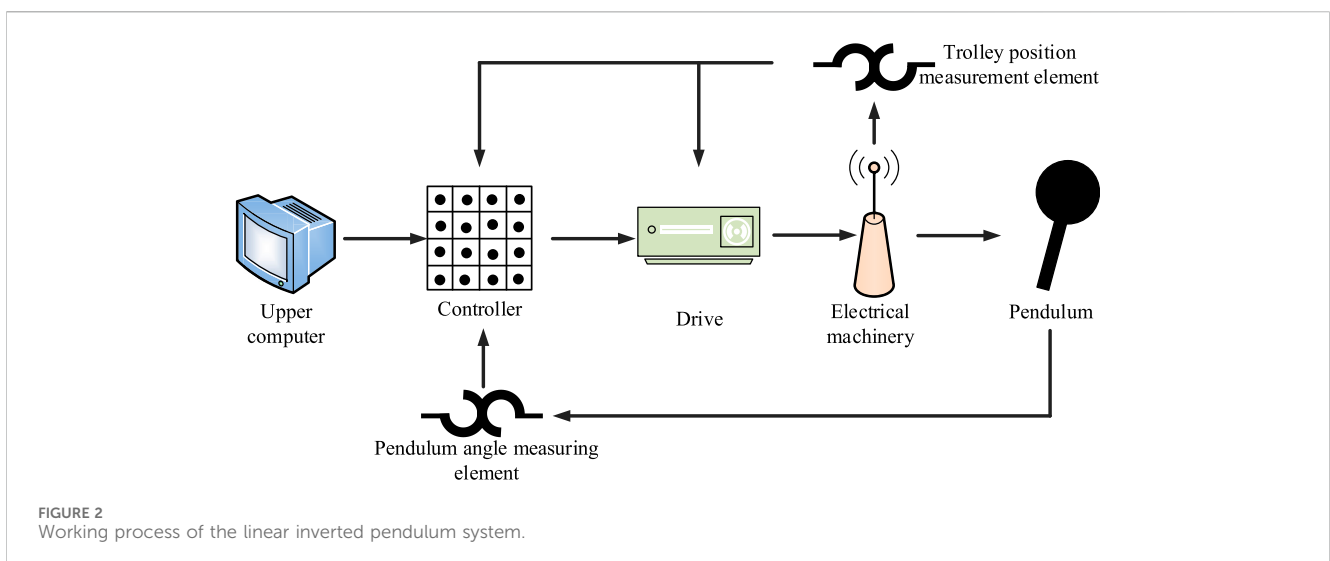


FIGURE 2 Working process of the linear inverted pendulum system.

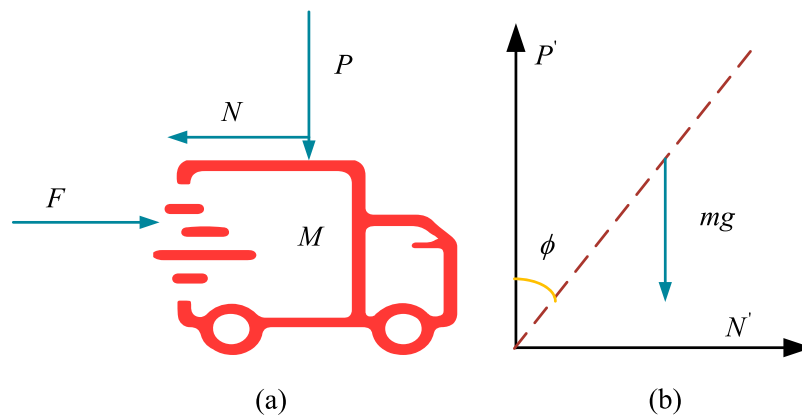


FIGURE 3 Force analysis of the small car and pendulum. (A) Force analysis diagram of the small car. (B) Analysis diagram of pendulum force.

utilized fuzzy logic to enhance the system resistance to changes and disturbances while optimizing the convergence efficiency of vibration mitigation and positioning errors. The performance of the proposed method was validated on the MATLAB/Simulink platform (Moudoud et al., 2022). To suppress the chattering effect and maintain robustness under load variation and parameter uncertainty, Kaplan O et al. proposed a second-order sliding mode control (SOSMC) to adjust the output voltage of DC/DC step-down converters by input cpll. The results show that the controller has high tracking accuracy and strong robustness, and can effectively reduce the chattering effect of the system under any input voltage or CPL power interference (Kaplan and Bodur, 2023).

In summary, although the above methods perform well under certain conditions, they may not be stable and robust enough to cope with sudden loads and parameter changes. For example, the control strategies in Sun et al. (2022) and Dong et al. (2023) have shortcomings in fast convergence and precise control. In Zhao et al. (2023) and Mendoza and Yu (2023), adaptive algorithms and fuzzy logic were used to improve the control accuracy, but i both needed improvement under strong interference. Chen et al. (2022) and Moudoud et al. (2022) performed well on trajectory tracking, but their methods may be unable to deal with complex systems and strong coupling problems. The overtorque control strategy proposed in Kaplan and Bodur (2023) still needs to improve the tracking accuracy and robustness under the conditions of load variation and parameter uncertainty. The advantage of this method is that it combines fuzzy adaptive technology and second-order sliding mode control to improve the robustness and adaptability of the system by dynamically adjusting the control gain and introducing the barrier Lyapunov function (BLF), which focuses on suppressing chatter and dealing with output constraints.

Inverted pendulum (IP) systems are a typical class of under-actuated mechanical systems that are multi-variable, high-order, non-linear, strongly coupled, and naturally unstable. IP is a typical algorithm validation platform in the field of control, which can effectively detect the feasibility and practical value of algorithms (Chotikunnan et al., 2022). Traditional SMCs perform well in dealing with non-linear systems, but the buffeting problem still exists. Under output constraints, it is difficult for traditional control

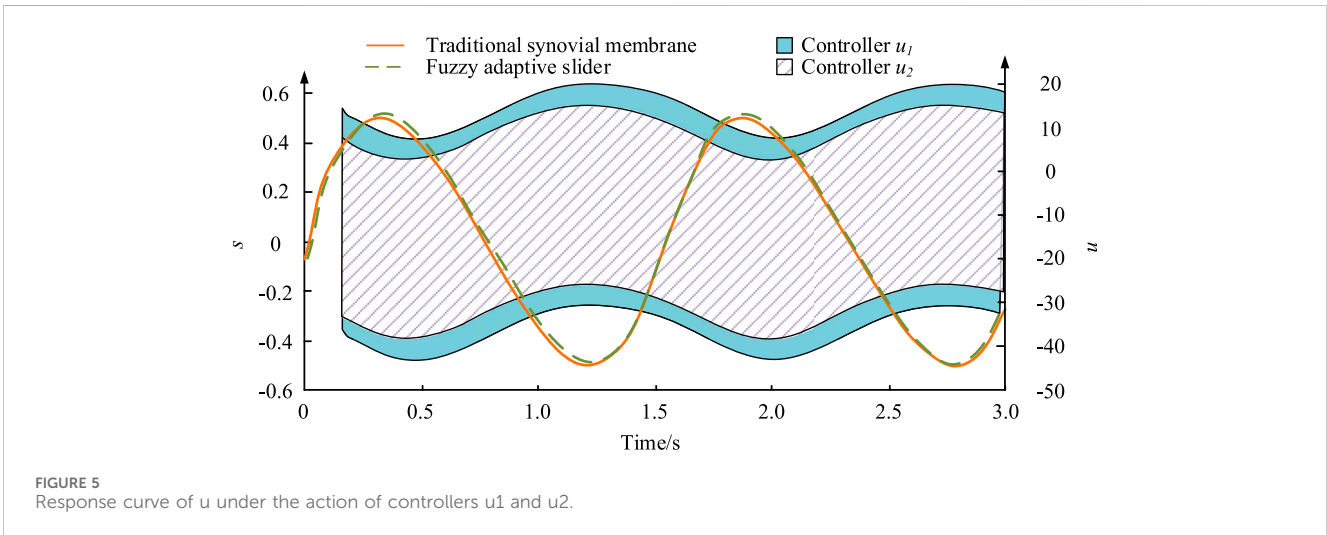
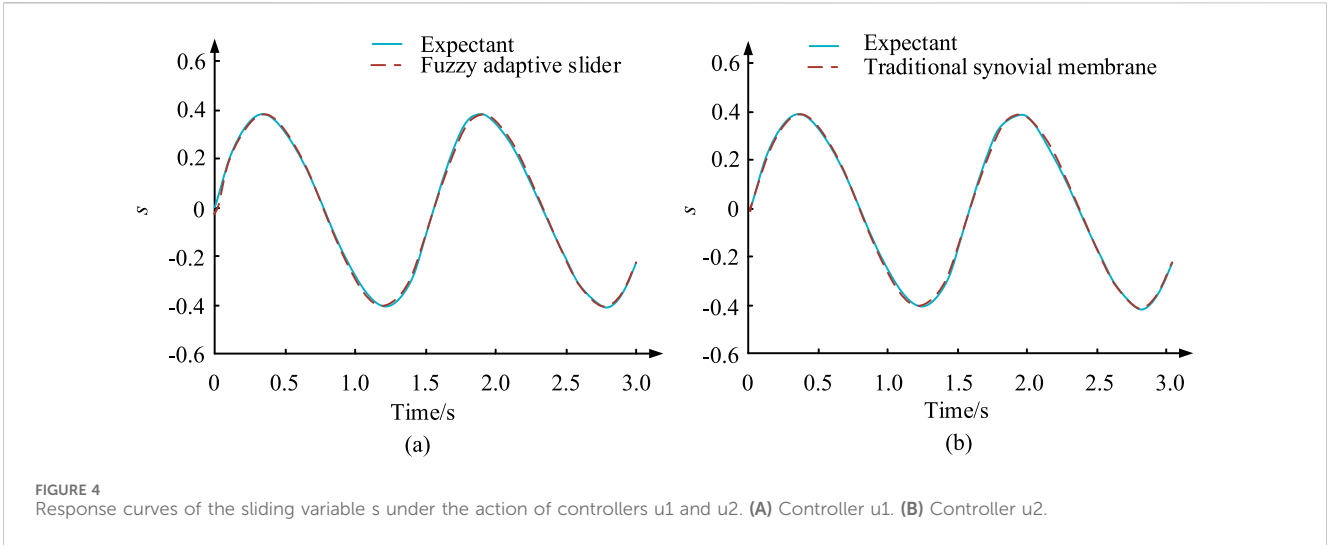
methods to ensure the stability of the system. In particular, in the fast-response scenario, the design complexity increases. It is usually necessary to combine fuzzy logic, adaptive mechanism, and other technologies. It is a typical under-actuated, highly non-linear, and unstable system commonly used to verify the effectiveness of control algorithms. In order to solve the uncertainty problem in non-linear systems, especially the inverted pendulum control problem, a second-order SMC combining fuzzy adaptive technique and the backstep method is designed. The fuzzy logic system is used to approximate the uncertainty, and the adaptive mechanism is used to adjust the control gain to ensure the stability and accuracy of the system. The effectiveness of the controller in the inverted pendulum system is verified under output constraints and unknown interference conditions.

The contribution of the research is as follows. In this paper, an innovative fuzzy adaptive second-order sliding mode control method is introduced, which combines the approximation ability of the fuzzy logic system with the robustness of second-order sliding mode control to provide new theoretical support for non-linear control systems. This method approximates the system uncertainty dynamically by fuzzy adaptive technology, effectively reduces the buffeting problem of traditional sliding mode control, and improves the smoothness and accuracy of control. To solve the problem of output limitation, the barrier Lyapunov function (BLF) technology is used to ensure that the system state converts to the equilibrium point within a limited time and does not exceed the predetermined constraints, which enhances the security and reliability. At the same time, the finite-time stability proof of the fuzzy adaptive second-order sliding mode controller is provided, which is crucial for predicting and understanding the system's behavior.

2 Methods and materials

2.1 The second-order sliding mode control method based on fuzzy adaptive control

Traditional SMC has attracted much attention due to its robustness to parameter changes and external disturbances in the field of control. In practical operation, due to factors such as the



component structure and the system itself, it is not possible to obtain an accurate mathematical model of the system in advance. This limits the applicability of traditional SMC in describing complex or difficult-to-quantify non-linear systems. The application of fuzzy logic can overcome this problem by estimating quasi unknown non-linear functions through language descriptions that rely on comprehensive expert experience. The study combines fuzzy control methods with robust adaptive laws to reduce the error between fuzzy approximation and actual readings. A fuzzy adaptive traditional SMC is constructed by approximating the unknown function of a non-linear system through a fuzzy logic system (FLS) and combining it with the traditional sliding mode. Figure 1 shows the proposed FLS.

In Figure 1, the fuzzy logic controller design mainly includes the following content: first, the input and output of the fuzzy controller are determined. Then, the control rules of the fuzzy controller are summarized. The methods for fuzzification and anti-fuzzification are determined. Second, the domain is chosen, and relevant

parameters are determined. The initial design can be simulated. If the control performance does not meet the requirements, the membership function needs to be redefined. Sometimes, the input/output quantities need to be redefined. The knowledge base based on fuzzy rules is composed of IF-THEN rules (Gauder et al., 2023). The multiple input single output (MISO) rule is used to formulate control laws (Soukkou et al., 2023). Based on the extension of implication in multi-valued logic, the implication rule using the t-norm operator is defined in Equation 1.

$$\mu_{A_1^i \times \dots \times A_n^i \rightarrow C^j}(X, y) = \mu_{A_1^i}(x_1) * \dots * \mu_{A_n^i}(x_n) * \mu_{C^j}(y). \quad (1)$$

In Equation 1, μ represents a fuzzy set. $X = (x_1, x_2, \dots, x_n)^T \in P \subset \mathbb{R}^n$ represents the input. $y \in Q \subset \mathbb{R}$ represents the output. A_i^j and B^j represent fuzzy sets. $*$ represents the t-norm. n represents the state number in a FLS. Fuzzification is a process of mapping a clear point into a fuzzy set B . Single-instance fuzzy mapping is shown in Equation 2.

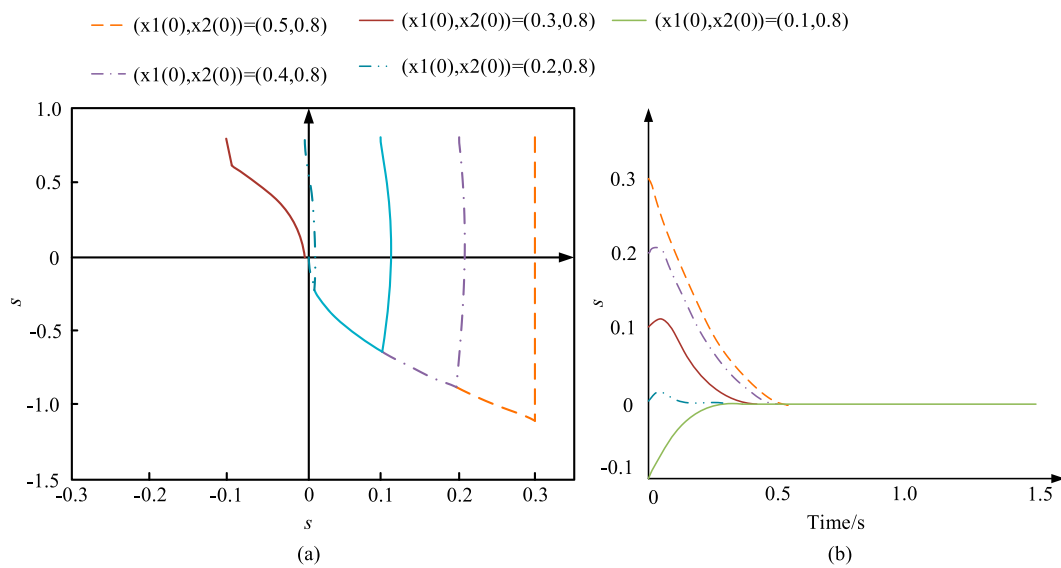


FIGURE 6 Phase plane trajectory and response curve of the controller during operation. (A) Phase plane trajectory of s - \dot{s} during the operation of the controller. (B) Response curve of s during controller operation.

$$\mu_B(X') = \begin{cases} 1, & X' = X \\ 0, & \text{others} \end{cases} \quad (2)$$

$$u^* = b^{-1}(-f(t, x) - h \cdot \text{sgn}(s) \cdot \eta\Delta), h = \begin{cases} 1, & s \neq 0 \\ 0, & s = 0 \end{cases} \quad (5)$$

Fuzzy reasoning is a mapping from a fuzzy set P to a fuzzy set R . Assuming that B is a fuzzy set in V , the fuzzy relationship formula is $B \circ R^j$. Product inference can be obtained using the t-norm operator and product operation. Defluzzing is the process of mapping a fuzzy set from R to a clear point in R . The central average method used is a FLS with a central average deblurring device, a product inference device, a singleton fuzzier, and a fuzzy basis function (FBF) (Ziyu et al., 2024). M represents the number of fuzzy sets. If μ_{A_i} is fixed and \bar{y}^i is considered an adjustable parameter, then $y(X) = \theta^T \xi(X)$, $\theta = (\bar{y}^1, \dots, \bar{y}^M)^T$. Before designing the FBF, all parameters in $\xi^j(X)$ can be fixed. The only variable parameter is θ . The FLS is used to construct a FBF with adaptive parameter vectors to replace unknown functions. To make the first-order non-linear system controllable, the tracking error is set to e , and the sliding surface is designed as $s = e$. From an initial condition $e = 0$, track issue $x = x_d$. x_d represents the expected state. All $t \geq 0$ maintain a state error vector on the sliding surface $s = e = 0$. By setting $s^2(e)$ as the Lyapunov function, the sliding condition can be replaced by Equation 3.

$$s \cdot \dot{s} \leq -\eta \cdot |s| \text{ or } s \cdot \text{sgn}(s) \leq -\eta. \quad (3)$$

After deriving Equation 3, Equation 4 can be obtained.

$$\begin{cases} \dot{s} = \dot{e} = f(t, x) + b(t, x)u, \\ f(t, x) = a(t, x) - \dot{x}_d(t). \end{cases} \quad (4)$$

In Equation 4, $a(t, x)$ and $b(t, x)$ both represent unidentified continuous functions. u represents the system input. Equation 5 is the SMC input u^* .

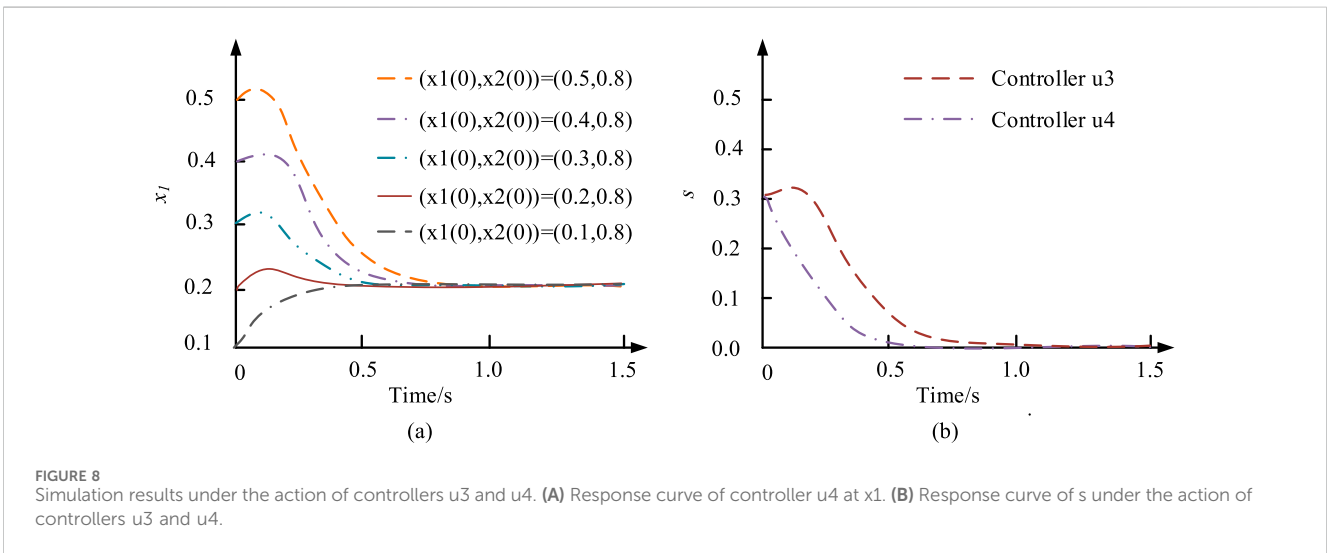
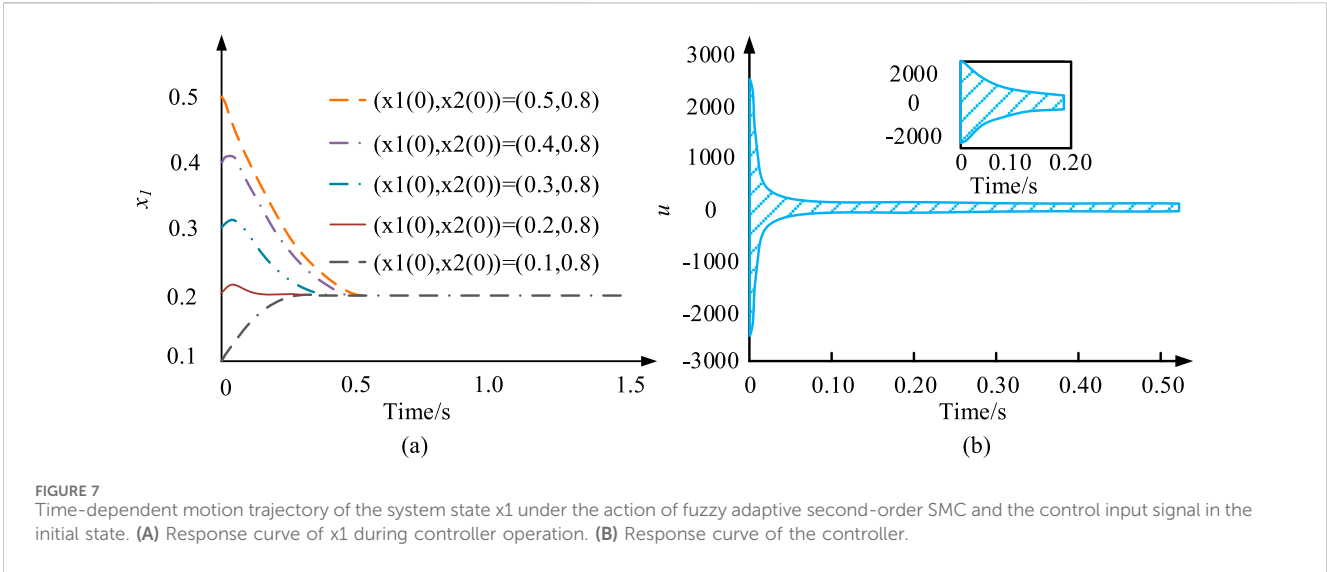
In most practical situations, functions $f(t, x)$ and $b(t, x)$ are in an unknown state. Therefore, an adaptive method for FLSs is proposed. $f(t, x)$ is replaced by FLS $\hat{f}(t, x)$. The disturbance caused by unknown control gain is reduced through $b^{-1} \text{sgn}(s)|A_1|$. Assuming that $0 < b \leq b(t, x)$ and $b(t, x) = B + \Delta b(t, x)$, B is a known normal number. $\Delta b(t, x)$ refers to an unidentified positive function. A controlling input in Equation 6 is obtained.

$$u_1 = B^{-1}(-f(x|\theta) - h \cdot \text{sgn}(s) \cdot \eta\Delta) - B^{-1} \text{sgn}(s)|A_1|. \quad (6)$$

θ^* is the optimal parameter vector for FLS. The upmost approximation error ω is defined. The Lyapunov function is $V_1 = \frac{1}{2}(s^2 + \frac{1}{\kappa_1} \phi^T \phi)$. κ_1 is a constant. By taking the derivative, Equation 7 is obtained.

$$\begin{aligned} \dot{V}_1 &= s\dot{s} + \frac{1}{\kappa_1} \phi^T \dot{\phi} \\ &= s\phi^T \xi(x) + s\omega - s \cdot h \cdot \text{sgn}(s) \cdot \eta\Delta + s\Delta b(t, x) \cdot B^{-1}A_1 \\ &\quad - s \cdot b(t, x)B^{-1} \text{sgn}(s)|A_1| + \frac{1}{\kappa_1} \phi^T \dot{\phi} \leq \frac{1}{\kappa_1} \phi^T (\kappa_1 \cdot s \cdot \xi(x) + \dot{\phi}) \\ &\quad + s\omega + s\Delta b(t, x) \cdot B^{-1}A_1 - |s| \cdot h \cdot \eta\Delta \\ &\quad - |s| \cdot b(t, x)B^{-1}|A_1| < \frac{1}{\kappa_1} \phi^T (\kappa_1 \cdot s \cdot \xi(x) + \dot{\phi}) + s\omega \\ &\quad - |s| \cdot h \cdot \eta\Delta - |s| \cdot |A|. \end{aligned} \quad (7)$$

In Equation 7, $\dot{\phi} = -\hat{\theta}$. According to the general approximation theorem, $s \cdot \xi$ is the order of magnitude of the maximum approximation error. In adaptive fuzzy systems, if ξ is not equal to 0, then ξ should be very small. Therefore, $\hat{\theta} = \kappa_1 \cdot s \cdot \xi(x)$ is



selected as the adaptive law. Assuming that the upper bound of ξ is unidentified, robust controlling means are contemplated. Equation 8 represents a control input design process at this time.

$$u_2 = B^{-1} \left(-\hat{f}(x|\theta) - h \cdot \text{sgn}(s) \cdot (\eta\Delta + \tilde{Q}) - B^{-1} \text{sgn}(s) |A_2| \right). \quad (8)$$

In Equation 8, $A_2 = (-\hat{f}(x|\theta) - h \cdot \text{sgn}(s) \cdot (\eta\Delta + \hat{\delta}))$, $\hat{\delta} = \partial^* - \tilde{\delta}$, $\partial^* = |\omega|_{\max}$. Assuming that the new Lyapunov function is $V_2 = \frac{1}{2} (s^2 + \frac{1}{\kappa_1} \phi^T \phi + \frac{1}{\kappa_2} \tilde{\rho}^2)$, the derivative of V_2 is taken. Equation 9 is the designed adaptive law.

$$\begin{cases} \dot{\theta} = \kappa_1 \cdot s \cdot \xi(x), \\ \dot{\tilde{\rho}} = \kappa_2 \cdot h \cdot |s|. \end{cases} \quad (9)$$

Equation 9 is substituted into the derivative of V_2 to obtain $\dot{V} \leq |s| \cdot h \cdot \eta\Delta$, which proves the asymptotic convergence of the system. The controller is designed as shown in Equation 10.

$$u_1 = B^{-1} \left(-\hat{a}(x|\theta) - h \cdot \text{sgn}(s) \cdot (\eta\Delta + \tilde{Q}) - B^{-1} \text{sgn}(s) \left| -\hat{a}(x|\theta) - h \cdot \text{sgn}(s) \cdot (\eta\Delta + \tilde{Q}) \right| \right). \quad (10)$$

The non-linear system $\dot{x} = f(t, x) + g(t, x)u$ is considered. x represents the system status. u_1 represents the control input of the system. $f(t, x) = 0.2x(t) - \sin(t) + e^{x(t)}$, $g(t, x) = 1.3|x(t)| \cdot \cos^2(x(t)) + 0.1$. The simulation verification is to design a controller to act on the system. Then, x can trace the signal $x_d = 0.5 \sin(4t)$. For FLS $\hat{a}(x|\theta)$, a first-order SMC is constructed for comparison, whose form is represented by Equation 11.

$$u_2 = -\frac{1}{B} (a(t, x) + h \cdot \text{sgn}(s) \cdot \eta\Delta). \quad (11)$$

The fuzzy logic system solves the uncertainty control problem of non-linear systems. Due to the estimation of system uncertainty, the controller gain selected does not need to be too large, thereby weakening the chattering caused by the traditional sliding mode. Based on the robust adaptive law, the error between actual uncertainty and fuzzy approximation is reduced to improve the system control accuracy and performance. To cope with the external interference caused by the magnetic field and improve the

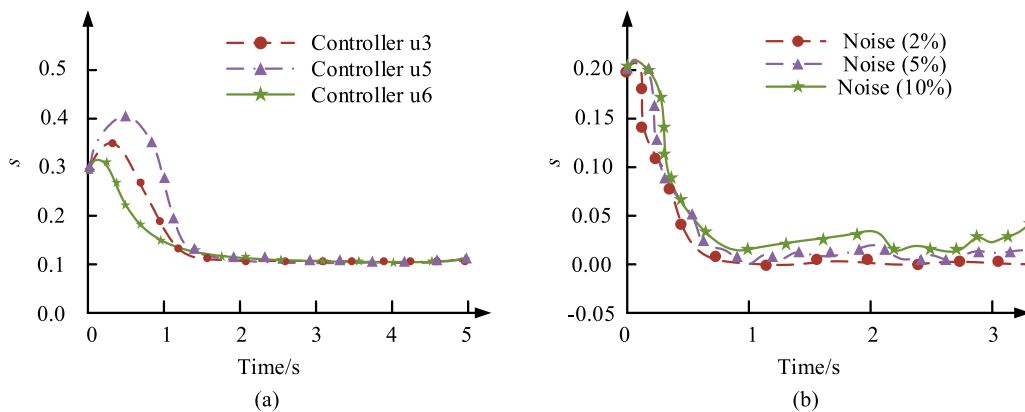


FIGURE 9 Simulation results of the system state under the action of controllers u3, u5, and u6. **(A)** Response curves of controllers u3, u5, and u6 at initial values $(x_1(0), x_2(0)) = (0.3, 0.8)$. **(B)** Response curve of s under the action of controller u3 with additional random noise (2%, 5%, and 10%).

robustness of the inverted pendulum system, the research method uses fuzzy logic rules to map the non-linear dynamics of the system to appropriate control parameters and then flexibly adjust them according to the current state changes. The control gain in real time is adjusted according to the different operating states of the system to improve the immunity. When the system state approaches the constrained edge, the controller increases the control input to prevent the state from deviating too much and avoid entering the unstable region. The process is completed by fuzzy logic reasoning, that is, the optimal control strategy is selected automatically according to the error and its change rate. The gain parameters are adjusted adaptively near the sliding mode surface to improve the control precision and system response speed. The optimized fuzzy adaptive SMC can realize precise control in a complex external environment and effectively resist non-linear factors such as magnetic field interference.

2.2 Fuzzy adaptive second-order sliding mode control means for the inverted pendulum system

Although the fuzzy adaptive first-order SMC strategy has some effectiveness in reducing oscillations, it still has shortcomings in eliminating vibrations compared with the second-order sliding mode. For uncertainties in non-linear systems, the traditional second-order sliding mode may no longer be applicable when there are safety and actuator structure limitations in the system. Output limitation is a challenge, which means that the system output must remain within a specific range. Otherwise, it may cause damage or performance degradation. To address these issues, research is being conducted to meet the requirement of system output limitation by referring to BLF. Then, adaptive fuzzy technology is used to dynamically approximate the uncertainty function. Finally, a new fuzzy adaptive second-order SMC is designed using adaptive control and power integral techniques. Fuzzy control has the powerful ability to approximate unknown terms in non-linear systems. The basic components of FLS include fuzzification,

fuzzy reasoning, and de-fuzzification (Guo and Zhao, 2023). Equation 12 is the single-instance fuzzification mapping used.

$$P_i(x) = e^{-\left(\frac{x_i - \vartheta_i}{Q_i}\right)^2} \quad (12)$$

In Equation 12, $Q_i, i = 1, 2, \dots, n$ represents the width of the function. ϑ represents a center vector. A_1^i, \dots, A_n^i and B^i represent fuzzy sets in U and V , respectively. $x_1 \in U \subset \mathbb{R}^n$ and $y \in V \subset \mathbb{R}$ represent the input and output variables of FLS, respectively. Equation 13 is the obtained FLS.

$$y(x) = \theta^T \psi(x) \quad (13)$$

In Equation 13, $\psi(x)$ represents the FBF. $\theta_{\bar{m}}$ and $\theta_{\bar{n}}$ represent adaptive parameter vectors. $\psi_{\bar{m}}(x)$ and $\psi_{\bar{n}}(x)$ represent fuzzy basis functions. \mathfrak{R} represents the compact region for x . Equation 14 is the minimum estimation error.

$$\hat{h} = (m(t, x) - \tilde{m}(x | \theta_{\bar{m}}^*)) + (n(t, x) - \tilde{n}(x | \theta_{\bar{n}}^*))v \quad (14)$$

In Equation 14, v represents the controlling item. Equation 15 is the fuzzy adaptive second-order SMC design process.

$$u = -\frac{1}{\tilde{n}(x | \theta_{\bar{n}})} \left[\frac{\beta_1}{12} \phi(s) \cdot \left[\dot{s}^{r_2} \right] + \beta_1^{\frac{a}{r_1}} [s]^{\frac{a}{r_1}} \right]^{\frac{r_3}{a}} + \tilde{m}(x | \theta_{\bar{m}}) + (\beta_2 + \gamma) \cdot \phi(s) \cdot \left(\left[\dot{s}^{r_2} \right] + \beta_1^{\frac{a}{r_1}} [s]^{\frac{a}{r_1}} \right) - \frac{\beta_2 + \gamma}{\tilde{n}(x | \theta_{\bar{n}})} \cdot \text{sign} \left(\left[\dot{s}^{r_2} \right] + \beta_1^{\frac{a}{r_1}} [s]^{\frac{a}{r_1}} \right) \quad (15)$$

In Equation 15, β_1 and β_2 represent appropriate normal numbers. $\phi(s) = \sec^2 \left(\frac{\pi |s|^{\frac{2a+r_1}{r_1}}}{s \delta^{\frac{2a+r_1}{r_1}}} \right)$. $\theta_{\bar{m}}$ and $\theta_{\bar{n}}$ are regulated using an adaptive law, as shown in Equation 16.

$$\begin{cases} \dot{\theta}_{\bar{m}} = Q_1 \left[[s]^{a/r_2} + \beta_1^{a/r_2} [s]^{a/r_1} \right]^{\frac{2a-r_3}{a}} \psi_{\bar{m}}(x), \\ \dot{\theta}_{\bar{n}} = Q_2 \left[[s]^{a/r_2} + \beta_1^{a/r_2} [s]^{a/r_1} \right]^{\frac{2a-r_3}{a}} \psi_{\bar{n}}(x)v. \end{cases} \quad (16)$$

v is shown in Equation 17.

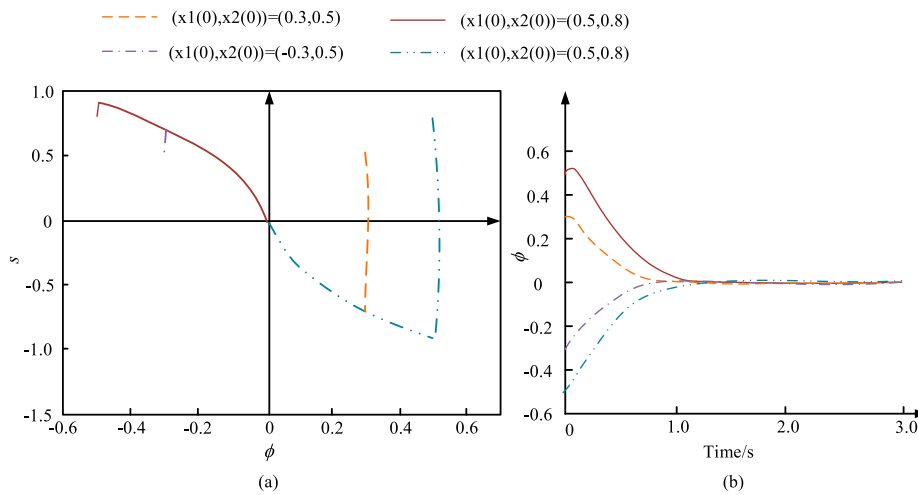


FIGURE 10 Simulation results of controller u_8 . (A) Phase plane trajectory of $s-\dot{s}$ during the operation of the controller. (B) Response curve under the action of controller u_8 .

$$v = -\frac{1}{\tilde{n}(x|\theta_{\tilde{n}})} \left[\tilde{m}(x|\theta_{\tilde{m}}) + \frac{\beta_1}{12} \phi(s) \cdot \left[[s]^{\frac{a}{r_2}} + \beta_1 \frac{a}{r_2} [s]^{\frac{a}{r_1}} \right]^{\frac{r_3}{a}} \right]. \quad (17)$$

In Equation 17, Q_1 and Q_2 represent normal numbers. At this point, the controller in Equation 9 ensures that the system satisfies the finite time stability of $s = \dot{s} = 0$. For all $t \geq 0$, a sliding variable s satisfies $|s| < \delta$. Parameters a and r_1 that satisfy $a \geq r_1$ are to prevent $\dot{V}(s_1, s_2, \tilde{\theta}_{\tilde{m}}, \tilde{\theta}_{\tilde{n}})$ singularity. If $r_1 > a$, $\frac{2a-r_3}{a}$ may be less than 1, and $\dot{V}(s_1, s_2, \tilde{\theta}_{\tilde{m}}, \tilde{\theta}_{\tilde{n}})$ is strange. When the sliding variable moves away from the origin, the larger the parameter a , the greater the control force provided by the controller, greatly improving the convergence ability of the closed-loop system. Parameters r_1, r_2, r_3 , and τ must conform to $r_2 = r_1 - \tau \geq 0, r_3 = r_2 - \tau \geq 0$, and $\tau > 0$. These conditions ensure the local homogeneity of $V(s_1, s_2, \tilde{\theta}_{\tilde{m}}, \tilde{\theta}_{\tilde{n}})$ and $\dot{V}(s_1, s_2, \tilde{\theta}_{\tilde{m}}, \tilde{\theta}_{\tilde{n}})$. This is also a sufficient and necessary condition for the stability of sliding variables within a finite time. The parameter β_1 cannot be selected too low because it will affect the convergence of sliding variables. If β_1 is large, the convergence speed of sliding variables will be faster. On the contrary, the convergence time of sliding variables is also longer. In addition, the parameter β_2 is restricted to meet $\beta_2 \geq c_1(\beta_1) + c_2(\beta_1)$. This requires $\beta_2 >$ a larger normal number as the control design employs a technique similar to backstepping, leading to an overestimation of β_2 (Jiang et al., 2023). The preset value of β_2 can be gradually reduced until a good performance of the closed-loop system is achieved. In other words, in practical operation, there is no need to be constrained by the above limitations as long as good performance can be achieved within a reasonable range. In addition, the parameter $\gamma > |\rho|_{\max}$ is helpful for the stability analysis of the adopted system. Moreover, $\tilde{m}(x|\theta_{\tilde{m}})$ and $\tilde{n}(x|\theta_{\tilde{n}})$ must accord with Equations 15, 17. The research mainly focuses on designing a fuzzy adaptive second-order SMC for non-linear systems having no output constraints. According to the actual situation, when the system does not consider constraints, $\phi(s) = 1$. In this case, the stability proof only needs to change BLF to Equation 18.

$$V_2(s_1, s_2) = \int_{s_2}^{s_1} \left[[\mu]^{\frac{a}{r_1}} - [s_1^*]^{\frac{2a-r_2}{a}} \right] d\mu. \quad (18)$$

In Equation 18, $s_1^* = 0$. First, the controlled variables of the IP system are determined to include the car position, car speed, pendulum angle, and pendulum angular velocity. Then, position information on the car and angle information on the pendulum are collected through measuring devices. The car speed and the angular velocity of the pendulum are calculated through corresponding calculations. The obtained information is transmitted to the controller and driver. The controller processes the received information into control variables and applies them to the motor, which, in turn, acts on the IP. The measuring device measures the car information again. The above processes are repeated until the pendulum can stabilize near the equilibrium position and continue to maintain a stable state. During the above process, the controller also transmits the measured information to the upper computer, which can intuitively observe various variables and make accurate analysis and judgments. Figure 2 shows the working process of the IP system.

Without considering air resistance, friction between components, and friction between the car and the ground, the linear first-level IP system can be simplified, as shown in Figure 3A. Figure 3B shows the force analysis of the car and the pendulum.

In Figure 3, F represents the force applied to the car. m_c is the mass of the small car. m is the mass of the pendulum. x represents the displacement of the small car. φ represents the angle between the pendulum and the vertical upward direction. l is the pendulum center and the distance of the rotation center. N and M represent the horizontal and vertical components of the interaction force between the car and the pendulum, respectively. N' and M' are equal to N and M in size, respectively, with opposite directions. Based on the above analysis, Equation 19 is a motion equation.

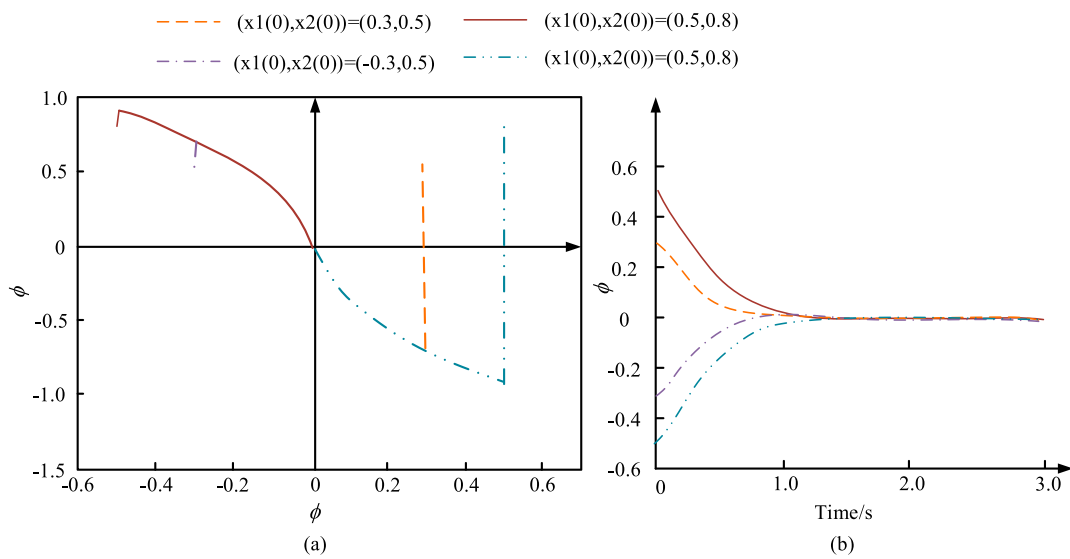


FIGURE 11 Simulation results of controller u_8 . (A) Phase plane trajectory of $s-s^{\cdot}$ during the operation of the controller. (B) Response curve under the action of controller u_7 .

$$(m_c + m)\ddot{x} - ml \cdot \dot{\phi}^2 \sin \phi = F. \tag{19}$$

Equation 20 is the torque balance equation for the pendulum.

$$P'l \sin \phi + N'l \cos \phi = I \frac{d^2 \phi}{dt^2}. \tag{20}$$

According to Lyapunov theory, the closed-loop dynamics of IP systems are finite-time stable. Equation 21 represents the fuzzy adaptive second-order mode controller u_3 and the second-order SMC u_4 without considering constraints.

$$\begin{cases} u_3 = v - \frac{25.1}{\hat{n}(x|\theta_n)} \cdot [\phi(s + \text{sign}([\dot{s}]^2 + 2.25[s]))], \\ u_4 = v - \frac{25.1}{\hat{n}(x|\theta_n)} \cdot \text{sign}([\dot{s}]^2 + 2.25[s]). \end{cases} \tag{21}$$

In addition, two second-order SMCs are constructed for comparison to demonstrate the superiority of the proposed algorithm. Equation 22 represents controllers u_5 and u_6 .

$$\begin{cases} u_5 = -\beta_2 \cdot \text{sign}\left([\dot{s}]^{\frac{\alpha}{r_2}} + \beta_1^{\frac{\alpha}{r_1}} [s]^{\frac{\alpha}{r_1}}\right) \\ u_6 = -(\beta_2^+ + \beta_2^- \bar{a}_{\max}(x)) \cdot \text{sign}\left([\dot{s}]^{\frac{\alpha}{r_2}} + \beta_1^{\frac{\alpha}{r_1}} [s]^{\frac{\alpha}{r_1}}\right) \end{cases} \tag{22}$$

Then, the reciprocal of time along the system is taken. Equation 23 is the design of the controller.

$$u_7 = v - \frac{9.1}{\hat{n}(x|\theta_n)} \cdot [\phi(s_1) + 1] \cdot \text{sign}(\xi_2). \tag{23}$$

A fuzzy adaptive second-order SMC u_7 without considering output constraints is constructed in Equation 24.

$$u_8 = v - \frac{9.1}{\hat{n}(x|\theta_n)} \cdot \text{sign}(\xi_2). \tag{24}$$

v is shown in Equation 25.

$$v = -\frac{1}{\hat{n}(x|\theta_n)} \left[\tilde{m}(x|\theta_n) + \frac{1.3}{12} \phi(s_1) \cdot \text{sign}(\xi_2) \right]. \tag{25}$$

The parameter vectors $\theta_{\tilde{m}}$ and $\theta_{\tilde{n}}$ satisfy the adaptive law of Equation 26.

$$\begin{cases} \theta_{\tilde{m}} = 6[\xi_2]^2 \psi_{\tilde{m}}(x), \\ \theta_{\tilde{n}} = 3[\xi_2]^2 \psi_{\tilde{n}}(x)v. \end{cases} \tag{26}$$

The fuzzy basis function is shown in Equation 27.

$$\psi_{l_1 l_2}(x) = \frac{\prod_{i=1}^2 \mu_{A_i^{l_i}}(x_i)}{\sum_{l_1=1}^7 \sum_{l_2=1}^7 \left(\prod_{i=1}^2 \mu_{A_i^{l_i}}(x_i) \right)}. \tag{27}$$

The proposed fuzzy adaptive second-order SMC is applied to IP systems in research. The proposed fuzzy adaptive second-order SMC is validated through an IP system. First, the model and force analysis of the traditional linear primary IP system are presented. Then, a fuzzy adaptive second-order SMC is designed for the IP system.

To sum up, the steps of fuzzy adaptive control design are as follows: first, the mathematical model of a non-linear system is established. Because of the uncertainties in the system, such as parameter change and external disturbance, it is difficult to describe them accurately by traditional control methods. Therefore, the fuzzy logic system is used to approximate these uncertainties. The input of the fuzzy logic system is usually the error or the error change rate, and the output is the control signal. The precise values are converted to fuzzy sets by fuzzification. Then, the central average method is

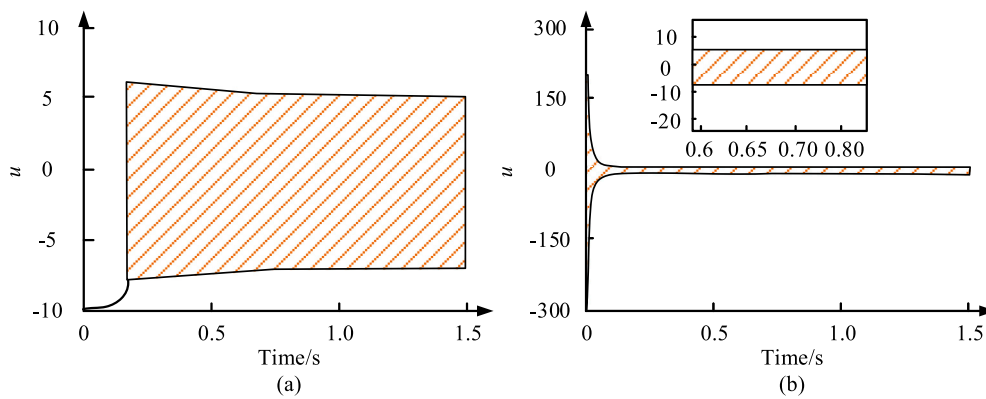


FIGURE 12 Response curves of u under the controllers u_7 and u_8 . (A) Response curve of u under the action of controller u_7 at initial values $(x_1(0), x_2(0)) = (0.5, 0.8)$. (B) Response curve of u under the action of controller u_8 at initial values $(x_1(0), x_2(0)) = (0.5, 0.8)$.

used for deblurring to obtain clear control values. The core is based on the IF-THEN rule base to deal with the uncertainty and non-linear problems, as well as fuzzy reasoning to achieve input–output mapping. The fuzzy controller adjusts parameters dynamically through the adaptive mechanism to improve the approximation accuracy. The design of the adaptive control law should be based on Lyapunov stability analysis to ensure the asymptotic stability of errors. In SMC, by defining the sliding surface and error, the fuzzy logic system is used to approach the uncertainty term, and fuzzy parameters are adjusted by an adaptive strategy to reduce the influence of error and uncertainty.

3 Results

3.1 Experimental analysis of the first-order sliding mode controller

The first-order SMC parameters are set as follows: $B = 2$, $\eta\Delta = 12$, $\kappa_1 = 5$, and $\kappa_2 = 6$. The initial state is $(x(0), \dot{x}(0)) = (-1, 0.8)$ and $\theta(0) = [0.8, \dots, 0.8]^T$. The sampling time is 0.0001s. Figure 4 shows the response curve of s .

In Figure 4A, the sliding variable can accurately track the dynamic expected value, with the maximum and minimum values of 0.4 and -0.4, respectively. Therefore, the feasibility of the proposed algorithm was demonstrated. In Figure 4B, based on SMC variables, it could accurately track and adapt to dynamically changing expected targets. The motion trajectories of sliding variables under the action of two controllers were compared together. This was to verify that the proposed fuzzy adaptive first-order sliding mode algorithm can inherit the robustness of traditional sliding modes. It can, to some extent, weaken the chattering generated by the traditional sliding mode. Figure 5 presents the results.

In Figure 5, the variation range of the traditional sliding mode and fuzzy adaptive slider was very similar, with both being within -0.5 – 0.5 . The designed fuzzy adaptive first-order SMC strategy exhibited the same robust characteristics as the traditional SMC. On the basis of achieving the same tracking

effect as the common goal, the vibration generated by the newly proposed controller u_2 was obviously lower than that when using the controller u_1 . The vibration of controller u_1 was within -35 – 19 and that of controller u_2 was within -45 – 19 .

3.2 Experimental analysis of the performance of second-order SMC

The parameters of fuzzy adaptive second-order SMC are set as follows: $\omega = 0.1$, $r_1 = 1$, $r_2 = 0.5$, $r_3 = 0$, $\beta_1 = 1.5$, $\beta_2 = 25$, $\tau = 0.5$, $Q_1 = 5$, and $Q_2 = 5$ to verify the effectiveness of fuzzy adaptive second-order SMC. The initial states are $(x_1(0), x_2(0)) = (0.5, 0.8)$, $(0.4, 0.8)$, $(0.3, 0.8)$, $(0.2, 0.8)$, $(0.1, 0.8)$, and $\theta_{\bar{m}}(0) = [0.8, \dots, 0.8]^T$, $\theta_{\bar{n}}(0) = [0.8, \dots, 0.8]^T$. The sampling time is 0.0001s. Figure 6 shows the phase plane trajectory and response curve of the controller during operation.

Figure 6A presents a phase trajectory of s - \dot{s} with various initial states under the action of fuzzy adaptive second-order SMC. Figure 6B shows the motion trajectory of the sliding variable s over time under the action of fuzzy adaptive second-order SMC. Figure 7A shows the motion trajectory of the system state x_1 over time under the action of fuzzy adaptive second-order SMC u_3 . Figure 7B shows the control input signal of controller u_3 in the initial state $(x_1(0), x_2(0)) = (0.5, 0.8)$.

Figure 7A shows that the sliding state s tracked the expected value. However, the system state x_1 did not cross the constraint boundary $|x_1| = \delta = 0.51$. When approaching the specified constraint boundary, the state x_1 was constrained within the boundary by the action of the controller. This could be obtained through the gain function $\phi(s)$. The value of the gain function was inversely proportional to the distance from state x_1 to the constraint boundary. In other words, as the system state x_1 approached the constraint boundary $|x_1| = \delta$, the value of the gain function became larger, providing greater control values to constrain the variables within the required range. Figure 7A shows that when the state x_1 approached the boundary, the control input signal became larger. Figure 8 shows the simulation results under the action of controllers u_3 and u_4 .

TABLE 1 Performance comparison results of each sliding mode controller.

Control method	Research method	Qiao and Wang (2024)	Mendoza and Yu (2023)	Chotikunnan et al., 2022
Accuracy/%	99.2	97.5	98.3	98.9
F1	0.95	0.87	0.91	0.93
Convergence time/s	1.25	2.52	1.84	1.53
Vibration range	0.1	0.4	0.3	0.2
Astringency/s	15	20	18	16

Figure 8A shows that under the initial condition $(x_1(0), x_2(0)) = (0.5, 0.8)$, the system state crossed the constraint boundary under the action of controller u4. Figure 8B shows when the state x_1 approached the constraint boundary, due to the significant force applied by the controller u3, the state x_1 crossed the constraint boundary. Under the action of controller u4, the system state x_1 crossed the constraining boundary. These results validate the advantages of the proposed controller u3. Figure 9 shows the simulation results of the system state x_1 under the action of controllers u3, u5, and u6.

Figure 9A shows the state x_1 reached stability under these controllers. If the control value of the controller u3 was smaller than that of the other two controllers, its sliding variable reached a stable state within 1.25 s, with a value of 0.1. This indicates that the proposed algorithm effectively reduces chattering. Figure 9B shows the sliding variable s affected by noise interference oscillated near the equilibrium point within a finite time. As the random noise applied to the system increased, the system performance also deteriorated.

3.3 Experimental analysis of fuzzy adaptive second-order SMC

The parameter settings are as follows: $a = r_1 = 2$, $r_2 = 1$, $\tau = 1$, $\beta_1 = 1.3$, $\beta_2 = 8.5$, $\gamma = 0.6$, $Q_1 = 6$, and $Q_2 = 3$ to validate the effectiveness of the fuzzy adaptive second-order SMC. The initial states are $\theta_a(0) = [0.6, \dots, 0.5]^T$ and $\theta_b(0) = [0.6, \dots, 0.6]^T$. The sampling time is 0.0001s. These initial conditions for selecting different IP systems are (0.3, 0.5), (-0.3, 0.5), (0.5, 0.8), and (-0.5, 0.8). Figure 10A shows the simulation results of controller u8.

Figure 10A shows the $s - \dot{s}$ phase trajectory under the action of controller u8. These sliding variables converged to a coordinate origin. Figure 10A shows the response curve of ϕ under the action of controller u8. The system state ϕ converged to 0 within a finite time at different initial values. When the initial values were $(x_1(0), x_2(0)) = (0.5, 0.8)$, ϕ crossed the constraint boundary in the initial response stage. Figure 11 shows the simulation results of controller u7.

Figure 11A shows the sliding variable converged to the coordinate origin. When the initial value was $(x_1(0), x_2(0)) = (0.5, 0.8)$, the system state ϕ did not cross the constraint boundary in the initial response. This is because when ϕ approaches the boundary, the function $\phi(s_1)$ will generate a large value that pulls ϕ back from the constraint boundary, ensuring that the variable does not cross the boundary. Figure 11B shows that under the action of controller u7, ϕ eventually reached the

equilibrium point within 15s. Figure 12 shows the response curve of u under the action of controllers u7 and u8.

According to Figure 12, for controller u7, at the beginning, u became large enough to constrain the state variable that was about to escape. After being constrained, u gradually decreased. As the system stabilized, u gradually stabilized within 10. To further verify the superiority of the research method, the performance of several SMCs was compared. The results are shown in Table 1.

From Table 1, the fuzzy adaptive second-order sliding mode controller (FASMC) designed in the research showed excellent performance in several indicators. In terms of accuracy, FASMC achieved 99.2%, which was significantly higher than that of other control methods in the literature. The F1 value of the research method was 0.95, indicating that FASMC was also superior to other methods in balancing accuracy and recall rate. The convergence time was only 1.25 s, which was faster than the method in the literature, indicating that the controller had a faster response in practical applications. In addition, the minimum vibration range of FASMC was only 0.1, which is far lower than that of other methods, demonstrating the advantages of the controller in terms of stability and its ability to effectively suppress flutter. Finally, the convergent state time of FASMC was 15 s, which was slightly shorter than that of other methods, further proving the efficiency of the method.

4 Discussion

This paper proposes a fuzzy adaptive second-order SMC method that significantly improves the control accuracy and system robustness, especially in suppressing chattering. Compared with traditional fuzzy sliding mode control, this method reduces the dependence on fixed gain by adjusting sliding mode gain adaptively and optimizes the control performance in a complex environment. Compared with the super-twisted sliding mode control in Chen et al. (2024), this paper achieves system stability within 1.25 s, and the speed is faster. In addition, this paper verifies its superior control effect in the inverted pendulum system, and it has a wide application prospect. Compared with the cascade sliding mode control in Dong et al. (2023), the adaptive fuzzy strategy proposed in this paper is more adaptable to system parameter changes and external disturbances. Although the stepped SMC performs well in scenarios such as anti-swing control of container gantry cranes, its adaptability and scalability are relatively insufficient. It is difficult to apply to complex systems. In this paper, the BLF is introduced to ensure the asymptotic stability under output constraints. The proposed method can converge quickly under different initial

conditions, and the state is always kept within the constraint range, showing excellent adaptability and anti-interference ability. The fuzzy adaptive SMC described in Moudoud et al. (2022) has a good effect in robot trajectory tracking, but its performance degrades with strong disturbance. In this paper, fuzzy logic and adaptive mechanism are used to reduce noise interference and ensure stable operation of the system. Finally, this paper converges the sliding mode variable to 0.1 within 1.25 s, and the control input is stable within 10, which is better than that of the methods in Kaplan and Bodur (2023) and Chotikunnan et al., 2022.

5 Conclusion

A control strategy was proposed to efficiently handle non-linear systems with uncertainty. This method first designed a first-order SMC based on fuzzy logic and an adaptive mechanism and analyzed its stability. It was further extended to second-order SMC. In addition, to address output limitation issues, BLF was introduced and applied to the actual system IP. In the simulation experiment, the new algorithm not only maintained the efficient performance of the control system but also tracked the sliding variable s over time under the action of fuzzy adaptive second-order SMC. In summary, first-order SMC sliding variables accurately tracked the dynamic expected value. Its maximum and minimum values were 0.4 and -0.4 , respectively. The sliding variable s converged within a finite time, thus proving the proposed algorithm's feasibility. The variation between the traditional method and fuzzy adaptive slider was similar, with both being within -0.5 – 0.5 . The vibration of controller u_1 was within -35 – 19 , and the vibration of controller u_2 was within -45 – 19 . This is because the fuzzy adaptive technology weakened the chattering problem in the traditional sliding mode to a certain extent. When the state x_1 approached the boundary, the control input signal became very large, which verified the effectiveness of the proposed controller. The state x_1 achieved its stability under these controllers. The control value of controller u_3 was smaller than that of the other two controllers. The sliding variable reached a stable state within 1.25 s, with a value of 0.1. This indicated that the proposed algorithm effectively reduced chattering. When the initial value was $(x_1(0), x_2(0)) = (0.5, 0.8)$, under the action of controller u_7 , the system state ϕ eventually reached the equilibrium point at different initial values. From the simulation results, the system converged quickly and had small oscillations. The state did not cross the constraint boundary. For controller u_7 , at the beginning, u became large enough to constrain the state variables that were about to escape. After being constrained, u gradually decreased. As the system stabilized, u gradually stabilized within 10. In system state convergence, there was no constraint boundary crossing, and the convergence speed was fast. Meanwhile, due to unknown system uncertainty, there was no need to consider controller design issues. The combination of fuzzy logic, adaptive mechanisms, and sliding

mode control increases design complexity, especially for fast responses. The adaptive mechanism reduces chatter, but the high-frequency switch increases actuator wear. The fuzzy logic system approximates non-linear function, reduces control gain requirement, and alleviates the flutter problem. BLF is introduced to ensure that the system state does not exceed the limit and the system is stable in a limited time. Therefore, the proposed algorithm has significant effectiveness in dealing with output constrained problems. Although the current algorithm is effective, there is still room for improvement. For example, intelligent technologies combining neural networks may further optimize the performance. This algorithm is successfully applied to linear IP systems. Therefore, in the future, this algorithm can be applied to a wider range of complex control systems, such as robots and drones.

Data availability statement

The original contributions presented in the study are included in the article/supplementary material; further inquiries can be directed to the corresponding author.

Author contributions

XL: conceptualization, data curation, formal analysis, investigation, methodology, project administration, resources, software, supervision, writing—original draft, and writing—review and editing.

Funding

The author(s) declare that no financial support was received for the research, authorship, and/or publication of this article.

Conflict of interest

The author declares that the research was conducted in the absence of any commercial or financial relationships that could be construed as a potential conflict of interest.

Publisher's note

All claims expressed in this article are solely those of the authors and do not necessarily represent those of their affiliated organizations, or those of the publisher, the editors, and the reviewers. Any product that may be evaluated in this article, or claim that may be made by its manufacturer, is not guaranteed or endorsed by the publisher.

References

- Chen, G., Jiang, Y., Guo, K., and Wang, L. (2022). Speed tracking control for unmanned driving robot vehicle based on fuzzy adaptive sliding mode control. *IEEE Trans. Veh. Technol.* 71 (12), 12617–12625. doi:10.1109/tvt.2022.3195608
- Chen, Q., Xiong, Z., Hu, Y., Huang, L., Liu, Q., and You, D. (2024). AFS control system research of distributed drive electric vehicles by adaptive super-twisting sliding mode control. *Trans. Inst. Meas. Control* 46 (7), 1388–1396. doi:10.1177/01423312231196400

- Dong, J., Sun, D., Jia, T., Sun, F., and Qin, Y. (2023). Research on anti-swing of container gantry crane as hierarchical sliding mode control. *J. Fail. Analysis Prev.* 23 (4), 1741–1751. doi:10.1007/s11668-023-01720-w
- Fei, J., Wang, Z., and Fang, Y. (2022). Self-evolving recurrent Chebyshev fuzzy neural sliding mode control for active power filter. *IEEE Trans. Industrial Inf.* 19 (3), 2729–2739. doi:10.1109/tii.2022.3162855
- Chotikunann, P., Chotikunann, R., Nirapai, A., Wongkamhang, A., Imura, P., and Sangworasil, M. (2023). Optimizing membership function tuning for fuzzy control of robotic manipulators using PID-driven data techniques. *J. Robot. Control* 4 (2), 128–140. doi:10.18196/jrc.v4i2.18108
- Gauder, D., Goelz, J., Jung, N., and Lanza, G. (2023). Development of an adaptive quality control loop in micro-production using machine learning, analytical gear simulation, and inline focus variation metrology for zero defect manufacturing. *Comput. Industry* 144 (21), 103799–103804. doi:10.1016/j.compind.2022.103799
- Guo, L., and Zhao, H. (2023). Online adaptive optimal control algorithm based on synchronous integral reinforcement learning with explorations. *Neurocomputing* 520 (2), 250–261. doi:10.1016/j.neucom.2022.11.055
- Jiang, S., Song, Y., Zeng, W., Zhang, H., Cai, S., and Lu, X. (2023). New results on adaptive fixed-time control for convex-delayed neural networks. *ISA Trans.* 134 (21), 134–143. doi:10.1016/j.isatra.2022.08.027
- John, Y. M., Sanusi, A., Yusuf, I., and Modibbo, U. M. (2023). Reliability analysis of multi-hardware–software system with failure interaction. *J. Comput. Cognitive Eng.* 2 (1), 38–46. doi:10.47852/bonviewjcc2202216
- Kaplan, O., and Bodur, F. (2023). Second-order sliding mode controller design of buck converter with constant power load. *Int. J. Control* 96 (5), 1210–1226. doi:10.1080/00207179.2022.2037718
- Kavikumar, R., Kwon, O. M., Lee, S. H., Lee, S. H., and Sakthivel, R. (2022). Input-output finite-time IT2 fuzzy dynamic sliding mode control for fractional-order nonlinear systems. *Nonlinear Dyn.* 108 (4), 3745–3760. doi:10.1007/s11071-022-07442-2
- Mendoza, A. M. E. R., and Yu, W. (2023). Fuzzy adaptive control law for trajectory tracking based on a fuzzy adaptive neural PID controller of a multi-rotor unmanned aerial vehicle. *Int. J. Control, Automation Syst.* 21 (2), 658–670. doi:10.1007/s12555-021-0299-2
- Moudoud, B., Aissaoui, H., and Diany, M. (2022). Fuzzy adaptive sliding mode controller for electrically driven wheeled mobile robot for trajectory tracking task. *J. Control Decis.* 9 (1), 71–79. doi:10.1080/23307706.2021.1912665
- Qiao, Y., and Wang, K. (2024). Fuzzy sliding mode speed control strategy of permanent magnet motor under variable load condition. *Int. J. Dyn. Control* 12 (5), 1616–1625. doi:10.1007/s40435-023-01285-4
- Soukkou, Y., Tadjine, M., Soukkou, A., Nibouche, M., and Nouri, H. (2023). Tuning functions based adaptive backstepping control for uncertain strict-feedback nonlinear systems using barrier Lyapunov functions with full state constraints. *Eur. J. Control* 70 (5), 100783–100810. doi:10.1016/j.ejcon.2023.100783
- Sun, X., Xiong, Y., Yang, J., and Tian, X. (2022). Torque ripple reduction for a 12/8 switched reluctance motor based on a novel sliding mode control strategy. *IEEE Trans. Transp. Electrification* 9 (1), 359–369. doi:10.1109/tte.2022.3161078
- Wu, T., Xue, K., and Wang, P. (2022). Leader-follower formation control of USVs using APF-based adaptive fuzzy logic nonsingular terminal sliding mode control method. *J. Mech. Sci. Technol.* 36 (4), 2007–2018. doi:10.1007/s12206-022-0336-y
- Zare, M., Pazooki, F., and Haghghi, S. E. (2022). Quadrotor UAV position and altitude tracking using an optimized fuzzy-sliding mode control. *IETE J. Res.* 68 (6), 4406–4420. doi:10.1080/03772063.2020.1793694
- Zhao, X., Gong, Y., Jin, H., and Xu, C. (2023). Adaptive super-twisting-based nonsingular fast terminal sliding mode control of permanent magnet linear synchronous motor. *Trans. Inst. Meas. Control* 45 (16), 3057–3066. doi:10.1177/01423312231162782
- Ziyu, G. U., Qiu, L., Pang, S., Zhou, W., Ji, C., and Zhang, C. (2024). Turbo-shaft engine adaptive neural network control based on nonlinear state space equation. *Chin. J. Aeronautics* 37 (4), 493–507. doi:10.1016/j.cja.2023.08.012